

## Cutting Gallium Oxide Nanoribbons into Ultrathin Nanoplates

Juan Xu,<sup>†</sup> Kwonho Jang,<sup>†</sup> Il Gu Jung,<sup>†</sup> Hae Jin Kim,<sup>‡</sup>  
Dong-Hwa Oh,<sup>§</sup> Joung Real Ahn,<sup>\*,§</sup> and Seung  
Uk Son<sup>\*,†</sup>

<sup>†</sup>Department of Chemistry and Department of Energy  
Science, Sungkyunkwan University, Suwon 440-746, Korea,  
<sup>‡</sup>Korea Basic Science Institute, Daejeon 350-333, Korea, and  
<sup>§</sup>BK21 Physics Research Division and SAINT, Sungkyunkwan  
University, Suwon 440-746, Korea

Received April 2, 2009

Revised Manuscript Received June 15, 2009

Inorganic nanomaterials having two-dimensional (2D) structural motifs have attracted the continuous attention of material scientists because of their promising electrical and physical properties<sup>1–8</sup> and have been applied as electrodes,<sup>2</sup> sensing materials,<sup>3</sup> and mechanical lubricants.<sup>4</sup> For fundamental studies or practical applications of 2D nanomaterials, the shape-controlled synthesis is crucial, as their properties are quite dependent on shape.<sup>1–8</sup>

Usually, 2D materials form plates, ribbons, and tubes, and recently, there has been significant progress in synthesis of nanoribbons and plates.<sup>1–8</sup> The most studied synthetic route for 2D nanomaterials is high temperature (600–1300 °C) chemical vapor deposition of a precursor

having a layer-structural motif.<sup>5</sup> In sharp contrast, colloidal synthesis of these materials in solution phase are relatively rare and still quite adventurous.<sup>6</sup> Moreover, as far as the authors are aware, there is no report on the shape-conversion of nanoribbons into plates in solution. Our research group has made continuous efforts to prepare ultrathin two-dimensional nanomaterials via colloidal chemical synthesis at relatively low temperature.<sup>7</sup> In this work, we report the wet-chemical synthesis of gallium oxide (Ga<sub>2</sub>O<sub>3</sub>) nanoribbons and their cutting into ultrathin nanoplates having a single-unit cell thickness by treatment with a sulfur solution.

Gallium oxide (Ga<sub>2</sub>O<sub>3</sub>) is a wide band gap (4.9 eV) material.<sup>8</sup> Its conductivity and optical properties are dependent on the oxygen vacancies in the crystal lattice.<sup>9</sup> On this basis, it has been applied in gas-sensor or optoelectronic devices.<sup>10</sup> Usually, gallium oxide has a monoclinic crystal system and forms one-dimensional materials such as nanowires.<sup>11</sup> Recently, Ga<sub>2</sub>O<sub>3</sub> nanoribbons have been prepared via catalyst-induced routes based on a vapor–solid (VS) method or vapor–liquid–solid (VLS) process at high temperatures.<sup>12</sup> However, as far as we are aware, there has been no report on the colloidal synthesis of gallium oxide nanoplates.

In a typical synthesis of gallium oxide nanoribbons, gallium chloride trihydrate (0.11 g, 0.48 mmol) was dissolved in well-dried oleylamine (4.0 mL) under nitrogen to form a transparent yellow solution. The temperature of the reaction mixture was increased to 230 °C at a rate of 3 °C/min. During the process, the solution became turbid and formed a white suspension. The reaction mixture was then cooled to room temperature. Excess methanol was added to the reaction mixture to induce precipitation of the white nanomaterial, which were retrieved by centrifugation. For transmission electron microscopy (TEM) analysis, a methylene chloride solution of the prepared nanomaterials was drop-casted on a grid. Figure 1 shows the typical TEM image of the prepared precipitates, in which ribbonlike materials were observed exclusively by measuring 244 samples with an average thickness of 1.45 ± 0.18 nm. Their powder X-ray diffraction (XRPD) pattern was indexed to the monoclinic-Ga<sub>2</sub>O<sub>3</sub>, JCPDS #11–370 (Figure 1b).<sup>13</sup>

\*Corresponding author. E-mail: sson@skku.edu (S.U.S.), jrahn@skku.edu (J.R.A.).

- (1) Reviews for nanomaterials having a 2D structural motif: (a) Tenne, R. *Angew. Chem., Int. Ed.* **2003**, *42*, 5124. (b) Rao, C. N. R.; Nath, M. *Dalton Trans.* **2003**, *1*. (c) Remskar, M. *Adv. Mater.* **2004**, *16*, 1497.
- (2) Tao, Z.-L.; Xu, L.-N.; Gou, X.-L.; Chen, J.; Yuan, H.-T. *Chem. Commun.* **2004**, 2080.
- (3) Law, M.; Kind, H.; Messer, B.; Kim, F.; Yang, P. *Angew. Chem., Int. Ed.* **2002**, *41*, 2405.
- (4) Rapoport, L.; Fleischer, N.; Tenne, R. *J. Mater. Chem.* **2005**, *15*, 1782.
- (5) Selected examples: (a) Nath, M.; Rao, C. N. R. *J. Am. Chem. Soc.* **2001**, *123*, 4841. (b) Ye, C.; Meng, G.; Jiang, Z.; Wang, Y.; Wang, G.; Zhang, L. *J. Am. Chem. Soc.* **2002**, *124*, 15180. (c) Brorson, M.; Hansen, T. W.; Jacobsen, C. J. H. *J. Am. Chem. Soc.* **2002**, *124*, 11582. (d) Chen, J.; Li, S.-L.; Tao, Z.-L.; Shen, Y.-T.; Cui, C.-X. *J. Am. Chem. Soc.* **2003**, *125*, 5284.
- (6) Selected examples: (a) Sigman, M. B. Jr.; Ghezelbash, A.; Hanrath, T.; Sanuders, A. E.; Lee, F.; Korgel, B. A. *J. Am. Chem. Soc.* **2003**, *125*, 16050. (b) Cao, Y. C. *J. Am. Chem. Soc.* **2004**, *126*, 7456. (c) Si, R.; Zhang, Y.-W.; You, L.-P.; Yan, C.-H. *Angew. Chem., Int. Ed.* **2005**, *44*, 3256. (d) Garje, S. S.; Eisler, D. J.; Ritch, J. S.; Afzaal, M.; O'Brien, P.; Chivers, T. J. *Am. Chem. Soc.* **2006**, *128*, 3120. (e) Huo, Z.; Tsung, C.-K.; Huang, W.; Fardy, M.; Yan, R.; Zhang, X.; Li, Y.; Yang, P. *Nano Lett.* **2009**, *9*, 1260.
- (7) (a) Park, K. H.; Choi, J.; Kim, H. J.; Oh, D.-H.; Ahn, J. R.; Son, S. U. *Small* **2008**, *4*, 945. (b) Park, K. H.; Choi, J.; Kim, H. J.; Lee, J. B.; Son, S. U. *Chem. Mater.* **2007**, *19*, 3861. (c) Park, K. H.; Jang, K.; Son, S. U. *Angew. Chem., Int. Ed.* **2006**, *45*, 4608.
- (8) (a) Hsieh, C.-H.; Chang, M.-T.; Chien, Y.-J.; Chou, L.-J.; Chen, L.-J.; Chen, C.-D. *Nano Lett.* **2008**, *8*, 3288. (b) Lee, S.-Y.; Gao, X.; Matsui, H. *J. Am. Chem. Soc.* **2007**, *129*, 2954. (c) Kisailus, D.; Choi, J. H.; Weaver, J. C.; Yang, W.; Morse, D. E. *Adv. Mater.* **2005**, *17*, 314. (d) Sun, X.; Li, Y. *Angew. Chem., Int. Ed.* **2004**, *43*, 3827. (e) Sharma, S.; Sunkara, M. K. *J. Am. Chem. Soc.* **2002**, *124*, 12288.

- (9) (a) Frank, J.; Fleischer, M.; Meixner, H. *Sens. Actuators, B* **1998**, *48*, 318. (b) Harwig, T.; Wubs, G. J.; Dirksen, G. J. *Solid State Commun.* **1976**, *18*, 1223.
- (10) (a) Edwards, D. D.; Mason, T. O.; Goutenoire, F.; Poeppelmeier, K. R. *Appl. Phys. Lett.* **1997**, *70*, 1706. (b) Ogita, M.; Saika, N.; Nakanishi, Y.; Hatanaka, Y. *Appl. Surf. Sci.* **1999**, *142*, 188.
- (11) (a) Chang, K.-W.; Wu, J.-J. *Adv. Mater.* **2004**, *16*, 545. (b) Chang, K.-W.; Wu, J.-J. *J. Phys. Chem. B* **2004**, *108*, 1838.
- (12) (a) Dai, Z. R.; Pan, Z. W.; Wang, Z. L. *J. Phys. Chem. B* **2002**, *106*, 902. (b) Choi, Y. C.; Kim, W. S.; Park, Y. S.; Lee, S. M.; Bae, D. J.; Lee, Y. H.; Park, G.-S.; Choi, W. B.; Lee, N. S.; Kim, J. M. *Adv. Mater.* **2000**, *12*, 746.
- (13) *Inorganic Phases*; JCPDS-International Centre for Diffraction Data: Swarthmore, PA, 1988.

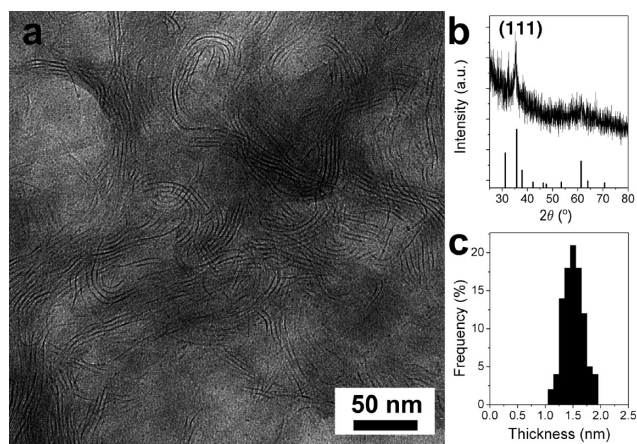


**Figure 1.** (a) Typical TEM image of the prepared gallium oxide nanoribbons, (b) XRPD pattern, and (c) thickness distribution diagram.

To investigate any transformation of the gallium oxide nanoribbons, they were treated with a sulfur solution at 230 °C, with the expectation of generating gallium sulfides. However, in actuality, the cutting of the gallium oxide nanoribbons into nanoplates was observed, maintaining the gallium oxide as main material (vide infra).

In a typical synthetic procedure of gallium oxide/gallium sulfide nanoplates, elementary sulfur (27.0 mg, 0.17 M) was dissolved in dried oleylamine (5.0 mL) and the reaction mixture heated to 230 °C. A hot gallium oxide solution was then injected into the sulfur solution. The reaction mixture was stirred at this temperature for 1 h and then cooled to room temperature. Excess methanol was added and the resultant precipitate retrieved by centrifugation. Images a and b in Figure 2 show the typical TEM images of the obtained materials. In a wide range of samples, well-assembled micro-sized wires were exclusively observed as shown in Figure 2a. In the magnified TEM image, good-quality nanoplates were observed as shown in Figure 2b. The thickness of the nanoplates was monodispersed with the average thickness and size measured as  $1.21 \pm 0.10$  and  $20.02 \pm 2.02$  nm, respectively. It has been well-documented that the unit-cell parameter of monoclinic-gallium oxide is 3.04, 5.80, and 12.21 Å, indicating that the thickness of the gallium oxide/gallium sulfide nanoplates prepared in this study corresponded to a single-unit cell thickness of  $\text{Ga}_2\text{O}_3$ .<sup>13</sup> High-resolution (HR)-TEM analysis showed that the (111) crystal plane is vertical to the plates. (see the Supporting Information). Unfortunately, the powder X-ray diffraction (XRPD) pattern of the nanoplates did not contain valuable information due to the ultrathin thickness of the materials. However, the heating of plates at 500 °C for 1 h showed the appearance of the  $\text{Ga}_2\text{O}_3$  peak. Energy-dispersive X-ray spectroscopy (EDS) of the obtained nanomaterials showed 6.0 atomic % of sulfur to gallium in the nanoplates (Figure 3a). Assuming that the gallium sulfide species was  $\text{Ga}_2\text{S}_3$ , the ratio of  $\text{Ga}_2\text{O}_3$ : $\text{Ga}_2\text{S}_3$  was calculated as 95.7:4.3 based on the EDS results. X-ray photoelectron spectroscopy also clearly supported that the main species was gallium oxide (Figure 3b). The

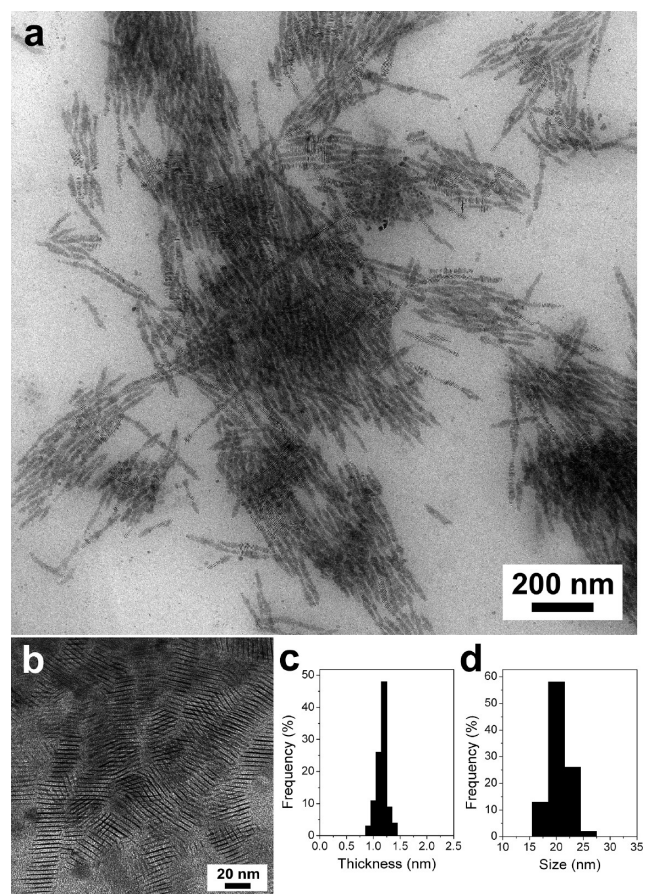


**Figure 2.** (a) Low-magnification, (b) high-magnification TEM images of gallium oxide/gallium sulfide nanoplates, and (c) thickness and (d) size distribution diagrams.

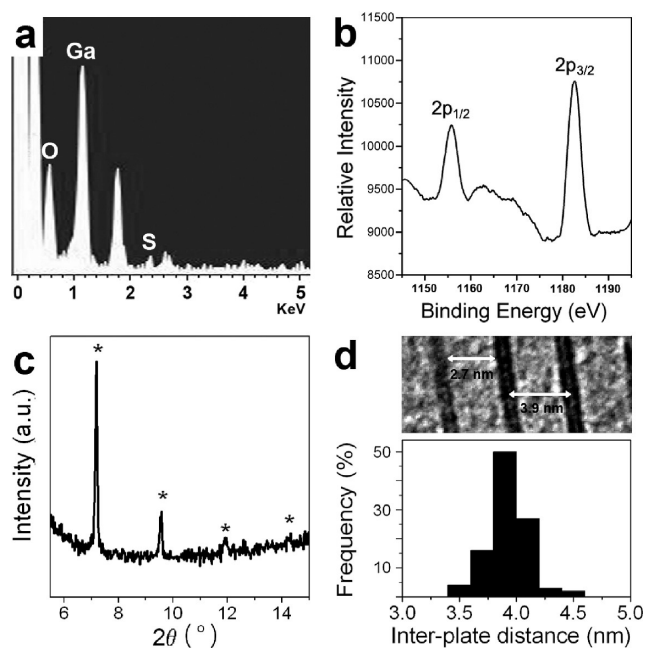


**Figure 3.** (a) EDS and (b) XPS spectra of gallium oxide/gallium sulfide nanoplates. (c) The powder X-ray diffraction pattern at small angle and (d) distance distribution diagram between nanoplates.

$2p_{3/2}$  gallium peaks at 1117.5 eV and the distance (26.8 eV) between the  $2p_{3/2}$  and  $2p_{1/2}$  peaks in the XPS spectra matched well with those of  $\text{Ga}_2\text{O}_3$  in the literature.<sup>14</sup>



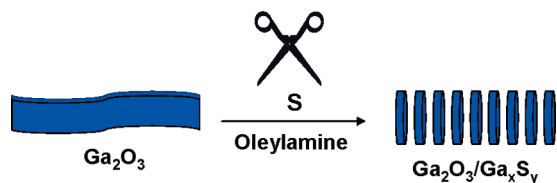


Figure 4. Cutting gallium oxide nanoribbons into nanoplates.

To consider the existence of the interaction between the plates, we statistically measured the distances between the plates with the help of TEM analysis. The average inter-plate distance of the assembled nanoplates was 3.9 nm by counting 100 distances. Also, the distance between the plates was calculated as 3.68 nm, based on the XRPD pattern at low angle, which matched the obtained value from TEM analysis, indicating that the colloidal nanoplates were completely separated by the surfactant molecules on surface. (Figure 3c–d and Figure S2 in the Supporting Information).

The quality of the prepared gallium oxide/gallium sulfide nanoplates was quite dependent on the concentration of the sulfur solution used. Nanoplates were exclusively observed in a 0.11–0.17 M concentration range of sulfur. Under optimized experimental conditions, a 0.17 M sulfur solution was used. Below 0.11 M, a mixture of nanoplates and ribbons was observed. When the same synthetic procedure was conducted without sulfur, nanoribbons were observed exclusively. When the concentration of sulfur was increased to 0.24 M, there were no detectable nanomaterials in the TEM image, possibly due to the small size of materials.

Considering that the obtained gallium oxide nanoribbons have an ultrathin thickness, one can expect the nanoribbons to be easily sliced via an appropriate chemical reaction (Figure 4). In the reaction of sulfur with gallium oxide, gallium sulfide would be partially formed and there would be an inevitable lattice mismatch between gallium oxide and gallium sulfide. To evaluate this mismatch effect, the structure of the sulfur atom-adduct to gallium oxide was simulated.<sup>15</sup> As displayed in Figure 5, three kinds of oxygen (O1, O2, O3) exist in monoclinic-Ga<sub>2</sub>O<sub>3</sub>. When the oxygens in the Ga–O1 (1.84, 1.95 Å), Ga–O2 (1.85, 1.93 Å), Ga–O3 (1.88, 2.01 Å) bonds were replaced with sulfur, the Ga–S bond lengths were simulated as 2.14 and 2.26 Å (Ga–S1), 2.16 and 2.22 Å (Ga–S2), and 2.14 and 2.26 Å (Ga–S3), respectively, with a structural distortion. We suggest that this significant mismatch could be a driving force in cutting nanoribbons into nanoplates.

It has been reported that gallium oxide nanomaterials, including nanoribbons, have many inevitable defects and oxygen vacancies within their structure.<sup>16</sup> The existence of defects in gallium oxide can be ascertained

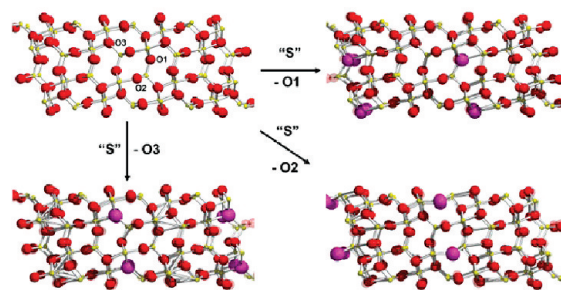


Figure 5. Simulated structure of the sulfur atom-adduct to gallium oxide; yellow, red, and violet balls represent Ga, O, and S, respectively.

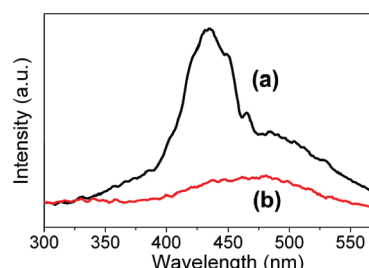


Figure 6. Emission spectra of gallium oxide nanoribbons (a) and gallium oxide/gallium sulfide nanoplates (b) obtained with a 250 nm excitation wavelength.

by observation of the photoemission.<sup>16</sup> Thus, if nanoplates were formed via reaction through defect sites with sulfur, a decrease in the emission properties would be expected. In this regard, the photoemission properties of nanoribbons and nanoplates was studied. In the literature, broad and irregular emissions of Ga<sub>2</sub>O<sub>3</sub> in the range of 400–500 nm with a 250 nm excitation wavelength have been reported.<sup>16</sup> Figure 6 shows the emission spectra of nanoribbons and nanoplates. The nanoribbons showed the complicated (but quite reproducible) emission band at 425–475 nm. In sharp contrast, this band disappeared in the emission spectra of the nanoplates, showing that the emission from defects was significantly decreased after transformation of nanoribbons into nanoplates.

We believe that the discovery of the cutting of the nanoribbons into nanoplates using sulfur solution can be applied to other diverse thin nanoribbons.

**Acknowledgment.** This work was supported by the Korea Research Foundation Grant funded by the Korean Government (MEST, KRF-2008-005-J00701). H.J.K. thanks the Hydrogen Energy R&D Center, a 21st century Frontier R&D Program.

**Supporting Information Available:** Details of experimental procedures and additional SEM and TEM images (PDF). This material is available free of charge via the Internet at <http://pubs.acs.org>.

- (14) Moulder, J. F.; Stickle, W. F.; Sobol, P. E.; Bomben, K. D. *Handbook of X-ray Photoelectron Spectroscopy*; Physical Electronics: Eden Prairie, MN, 1995.
- (15) See the Supporting Information for details.

- (16) (a) Kim, H. W.; Kim, N. H.; Lee, C. J. *Mater. Sci. Mater. Electron.* **2005**, *16*, 103. (b) Fu, L.; Liu, Y.; Hu, P.; Xiao, K.; Yu, G.; Zhu, D. *Chem. Mater.* **2003**, *15*, 4287. (c) Binet, L.; Gourier, D. *J. Phys. Chem. Solids* **1998**, *59*, 1241. (d) Harwig, T.; Kellendonk, F. *J. Solid State Chem.* **1978**, *24*, 255.